NASA TM-76687

NASA TECHNICAL MEMORANDUM

NASA TM-76687

NASA-TM-76687 19820012318

SONIC WIND TUNNEL OF THE INSTITUTE OF FLUID MECHANICS OF LILLE

G. Gontier

Translation of "Soufflerie sonique de l'Institut Mécanique des Fluides de Lille", La Recherche Aéronautique, no. 10, 1949, pp. 3-9.

NATIONAL AERONAUTICS AND SPACE ADMINISTRATION
WASHINGTON, D.C. 20546 MARCH 1982

STANDARD TITLE PAGE

1. Report No. NASA TM-76687	2. Government Accession No.	3. Recipient's Catalog No.
4. Title and Subtitle SONIC WIND TUNNEL OF THE INSTITUTE OF FLUID MECHANICS OF LILLE		5. Report Date March 1982 6. Performing Organization Code
7. Author(s) G. Gontier Office National d'Etudes et des Recherches Aéronautique		8. Performing Organization Report No. 10. Work Unit No.
9. Performing Organization Name and Address Leo Kanner Associates Redwood City, California 94063		11. Contract or Grant No. Nasw-3541 13. Type of Report and Period Covered Translation
12. Sponsoring Agency Name and Address National Aeronautics and Space Administration, Washington, D.C. 20546		14. Sponsoring Agency Code

15. Supplementary Notes
Translation of "Soufflerie sonique de l'Institut Mécanique des Fluides de Lille", La Recherche Aéronautique, no. 10, 1949, pp. 3-9.

16. Abstract
The author describes a 65 hp wind tunnel with a 40 mm by 240 mm airstream. This wind tunnel can achieve speeds in the neighborhood of the speed of sound, both subsonic and supersonic. It is useful in studying the transonic bump technique. The test section is 600 mm long. The side walls are made of transparent glass, and both the upper and lower walls are deformable, each through the use of nine jacks with elastic sleeves. So as to avoid condensation, the airstream's temperature is stabilized by an air exchanger at the temperature of the outside air. The author also gives the first results for supersonic operation, the distribution of Mach numbers within the airstream between the parallel walls, the value of the use factor, and the diffuser's efficiency.

17. Key Words (Selected by Author(s))	18. Distribution Statement
	Unlimited-Unclassified

19. Security Classif. (of this report)	20. Security Classif. (of this page)	21. No. of Pages	22.
Unclassified	Unclassified	15	

N82-20192#

SONIC WIND TUNNEL OF THE INSTITUTE OF FLUID MECHANICS OF LILLE

G. Gontier

Research Engineer at ONERA

The R and D work for this wind tunnel was carried to a successful conclusion thanks to the collaboration of the personnel at the Lille Institute of Fluid Mechanics, particularly that of Messrs. Maurice Dubois and Jean-Marie Olive, and of Mr. François Warlop and his crew of mechanics. /3*

Summary

The author describes a 65-horsepower wind tunnel with a rectangular airstream measuring 40 mm by 240 mm. This wind tunnel can achieve speeds in the neighborhood of the speed of sound, both subsonic and supersonic. It is useful in studying the transonic bump technique. The test section is 600 mm long. The side walls are made of transparent glass, and both the upper and lower walls are deformable, each through the use of nine jacks with elastic sleeves. The temperature is stabilized by an air exchanger. So as to avoid condensation, the airstream's temperature is allowed to go up to that of the outside air.

The author gives the first results for supersonic operation, the distribution of Mach numbers within the airstream between the parallel walls, the value of the use factor, and the diffuser's efficiency.

1. Introduction

In order to have the capacity to explore the transonic domain, the Office National d'Etudes et de Recherches Aéronautiques [ONERA -- the National Office for Aeronautical Research and Study] decided on April 15, 1947, to construct a small wind tunnel in the laboratories

*Numbers in the margin indicate pagination in the foreign text.

of the Lille Institute of Fluid Mechanics that could attain and even slightly surpass the speed of sound through the use of a 65 hp three-phase wound rotor electric motor, which was available at that time.

Our goal during the project was to create a uniform flat flow in which the Mach number might attain a value on the order of 0.9 in a rather long test chamber with a rectangular cross section that was as large as possible. As far as the technical study of the facility's various components went, we attempted to produce a tool that did not take up much space, was easily controllable, and could be rapidly and inexpensively altered. To make the working conditions more comfortable, we tried to attenuate the vibrations, eliminate the noise, and keep the temperature within a bearable range, considering what the technical requirements were.

The purpose of this report is to describe the Lille sonic wind tunnel, give its main characteristics, list the principles of the aerodynamic scheme, and publicize the most important results.

2. Brief Description of the Wind Tunnel

The wind tunnel is a return-flow one. It is installed in a room that is large enough to use state of the art methods of visualization: schlieren photography and shadowgraphs (figure 1).

The test chamber, 600 mm long with a 40 x 240 mm rectangular cross section at its entrance, has deformable top and bottom walls (figure 2). On the sides are two glass plates 30 mm thick. These walls slightly diverge to correct for boundary layer effects and /4 obtain a uniform longitudinal distribution of speed. The deformable top and bottom are controlled by 14 jacks with elastic sleeves (figures 5 and 6). This arrangement has the advantage of eliminating the connecting rods in conventional systems.

Regulation and stabilization of speed in the airstream are obtained through the use of a deformable sonic throat placed down-

stream from the chamber and controlled by four jacks identical to those in the test chamber.

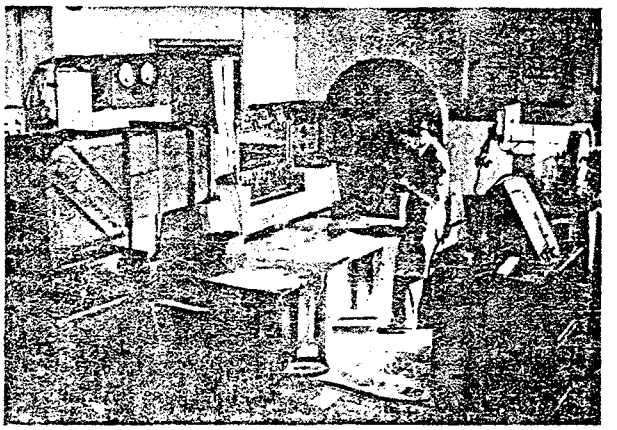

Figure 1
General View of the
Sonic Wind Tunnel

The collector, made of casted and machined aluminum alloy, has a profile formed of cubic arcs. The sectional contraction ratio is 26.

The air is put in motion by a centrifugal fan which produces a flow of 2.3 m^3/sec with a compression ratio of 1.13:1. The 1 meter diameter rotor is driven by a 65 hp three-phase wound rotor induction motor running at a rotational speed that is adjustable between 1000 and 2900 rpm.

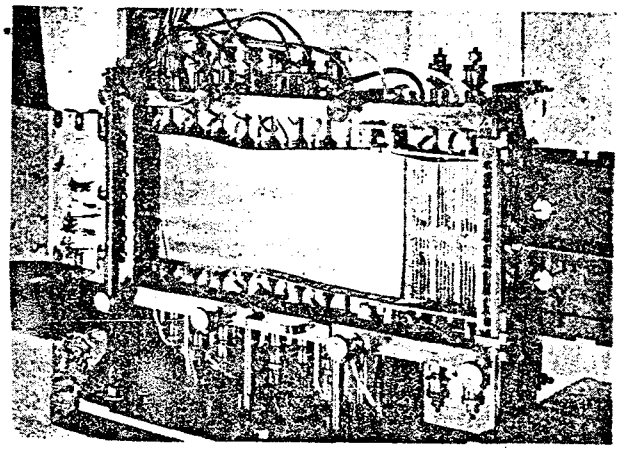

Figure 2
Deformable Walled
Experiment Chamber

Dust is removed from the moving air by greasing the vanes in the elbow of the fan exhaust. These vanes are mounted on a removable frame. Cleaning them is easy.

Cooling is accomplished by means of an adjustable air exchanger. It can be reinforced by circulating cold water in the hollow vanes in the large elbows of the return circuit (figure 3).

The air exchanger is adjusted so as to establish a chamber temperature that is at least equal to that of the air entering the

wind tunnel. Condensation and frosting inside the experiment chamber are thus avoided.

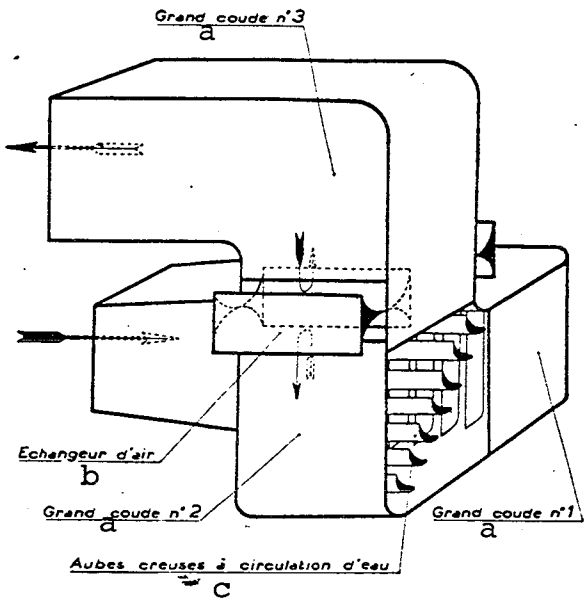

Figure 3
Large Elbows and their Vanes
Air Exchanger

Key:

a) Large Elbow
b) Air Exchanger
c) Hollow Vanes for Circulating Water

To attenuate noise and vibrations, the channel is divided up into a large number of short sections connected by thick rubber joints. The parts of the circuit in which the air speed exceeds 200 m/sec have been reinforced. The test chamber and the motor-fan assembly are supported by elastic suspensions, each resting on a heavy reinforced concrete block. In this way, the ground and the optical instruments it supports hardly vibrate at all.

3. The Wind Tunnel's Thermodynamic Scheme

The choice of wind tunnel type imposes the following givens:

-- The plenum chamber's pressure is equal to atmospheric pressure because of its closeness to the air exchanger.

-- The test chamber's temperature is equal to the outside temperature, i.e. about 15°C, so as to avoid any condensation.

-- The airstream's Mach number is equal to 0.9.

To determine the aerodynamic elements along the portion of the channel in which the flow can be considered isentropic, we graphically represented the variations in absolute temperature θ, density ρ, and

pressure p relative to the generating conditions, the variations in speed V relative to the limiting speed U, and the variations of the flow cross section σ relative to the sonic throat σ_c all as a function of Mach number M. While assuming the conditions mentioned above, we also traced the variations in speed V_o, the dynamic pressure, $\rho_o V_o^2/2$, and the kinetic power per unit of cross sectional area, $\rho_o V_o^3/2$, in the airstream as a function of the stream's Mach number M_o. Notice that the dynamic pressure and the kinetic power have maxima, the former at $M_o = \sqrt{2}$, independent of the circulating fluid, and the latter at $M_o = \sqrt{6/(3-\gamma)}$.

While evaluating the load losses in the various wind tunnel components, it appeared to us that the area of the airstream cross section adapted to a power of 65 hp was approximately 1 dm^2: We chose a rectangular cross section with a length to width ratio of 6 and the dimensions of 40 x 240 mm, which gives an area of 0.96 dm^2 and a flow of 2.14 kg/sec.

Before choosing the fan, the required compression ratio still has to be determined. We evaluated the wind tunnel's use factor η_s by making comparisons with similar wind tunnels whose results are known. The value $\eta_s = 5$ was adopted. Experience subsequently showed that this value was too high and that it would have been more prudent to use half that value. It is known that the difference in pressure at the fan under these conditions has to be 630 mm of water. We thought that it would be prudent to double this result, and our choice centered on a centrifugal fan that, at a speed of 2900 rpm, gives a flow of 2.3 m^3/sec with a pressure difference of 1370 mm of water and a power requirement of 65 hp.

It was very important to precisely calculate the divergence of the test chamber's side walls so as to correct for the boundary layer effects and obtain a uniform longitudinal speed distribution. To determine the width b_1 at the sonic throat, i.e. 800 mm from the entrance to the test chamber, we used five methods whose results were then compared. /5

A calculation of the width of displacement of the boundary layer, assumed to be turbulent throughout the chamber yielded b_1 = 45.2 mm. We obtained b_1 = 45.0 by using the boundary layer readings made in one of the intermittent wind tunnels at the Centre d'Essais de Mécanique des Fluides (Paris) [Center for Fluid Mechanics Experiments].

H. W. Liepmann's wind tunnel [3] at GALCIT (USA) is a facility that is very similar to the one at Lille. The test chamber, which is rectangular and has a height to width ratio of 10, goes from a width of 2 inches to 2.21 inches over a length of 36 inches. The Mach number, equal to 0.85 at the chamber entrance, increases by 2.5% in the exit section. The relative variation in cross sectional area:

$$\frac{d\sigma}{\sigma} = \frac{M^2 - 1}{\frac{\gamma - 1}{2} M^2 + 1} \frac{dM}{M}$$

shows that to keep M constant it would have been necessary to increase the width by 0.5%, i.e. adopt a value of 2.22 inches. As the thickness of a turbulent boundary layer is proportional to the 0.8 power of the distance from the leading edge, we find that the width b_1 in the Lille wind tunnel has to be 45.35 mm. Furthermore, taking account of friction, the increase in width must be proportional to the chamber's length, the square of the Mach number, and the hydraulic radius, i.e. to the area σ divided by the perimeter of the perpendicular cross section. We thus find a value for b_1 of 45.5 mm.

Lastly, we can also calculate b_1 by applying the theory of partitioned flow with friction along the chamber [1]. The speed remains constant if the dihedral angle of the side walls is equal to:

$$\frac{\gamma c_t}{2 r} b M^2$$

where c_t is the coefficient of friction, which can be estimated to be 0.005 in the present case, and r is the hydraulic radius. We

obtain b_1 = 45.3 mm. The first two results were rather uncertain and gave only an order of magnitude. We therefore adopted a value close to the average of the last three results, or 45.4, as the width of the sonic throat exhaust.

By circulating water in the 21 vanes in the return circuit elbows, one can absorb each second a quantity of heat equivalent to a power of 7 hp [4]. As this result is insufficient, we installed an air exchanger [5] upstream from the plenum chamber. It is made up of two biconcave blocks that enter the channel through two lateral rectangular openings. These blocks divert part of the hot air into the outside atmosphere. They also guide the intake of fresh air coming from the room (figure 3).

The power required to start the newly injected air moving is only about 0.04 hp. We neglect this figure and write that after temperature stabilization, all the power supplied to the fan is equal to the reduction in enthalpy experienced by the air when crossing the exchanger. After having made all the calculations, we obtain:

$$\frac{\frac{\gamma-1}{2}M^2_0}{\frac{\gamma-1}{2}M^2_0+1} = \eta_s \frac{k}{1-k}\left(1-\frac{\Theta_a}{\Theta_i}\right)$$

where M_o is the Mach number in the airstream, k the fraction of air exchanged, and Θ_i and Θ_a the absolute temperature of the air in the plenum chamber and the air introduced by the exchanger. This equation is graphically solved by letting:

$$\mu = \frac{\frac{\gamma-1}{2}M^2_0}{\frac{\gamma-1}{2}M^2_0+1}$$

$$\lambda = \frac{k}{1-k}\left(1-\frac{\Theta_a}{\Theta_i}\right)$$

and tracing the curve μ as a function of the family of lines $\mu = \eta_3\gamma$ representing different values of η_s, and the family of lines $\lambda = \frac{k}{1-k}\left(1-\frac{\Theta_a}{\Theta_i}\right)$ plotted as a function of Θ_a/Θ_i and representing different values of k (figure 4).

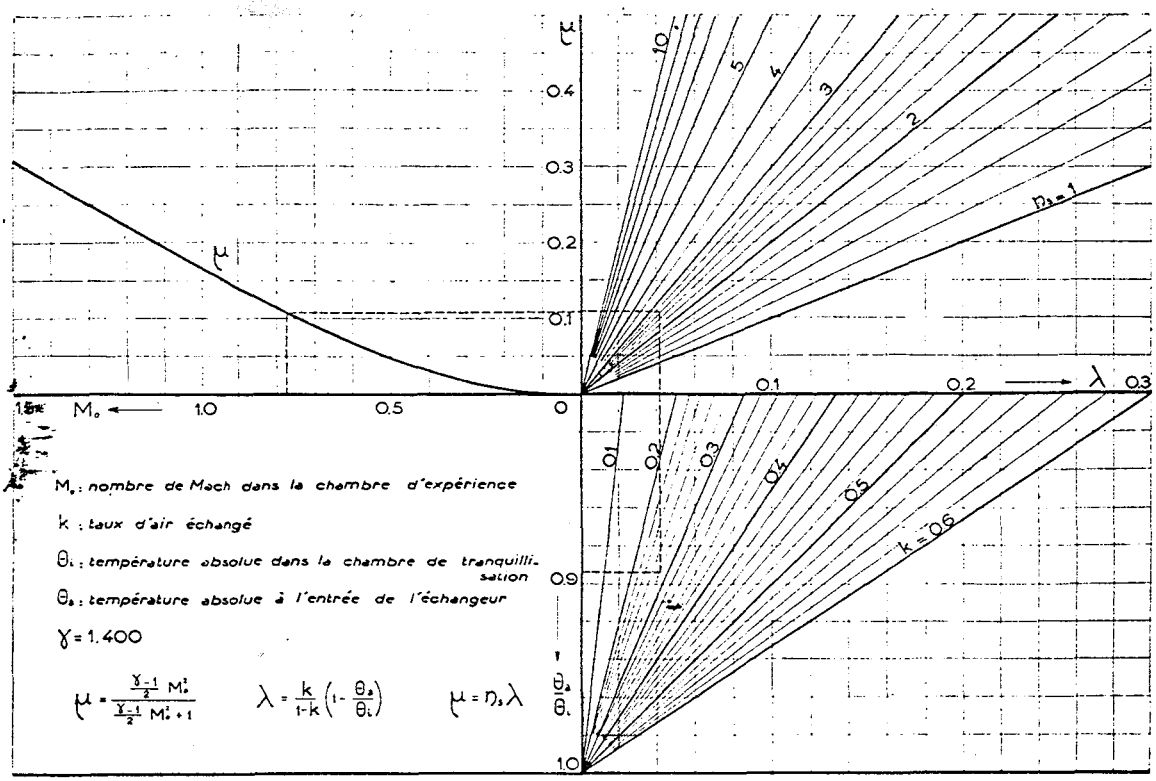

Figure 4
Air Exchange Cooling Chart

Key: M_o: Mach number in the test chamber
k: Fraction of air exchanged
θ_i: absolute temperature in the plenum chamber
θ_a: absolute temperature in the exchanger intake

4. Description of Some Subassemblies

The shape of the deformable walls of the test chamber and sonic throat is controlled through the use of jacks that must possess /6 two degrees of freedom. The two-directional control is achieved conventionally with a shaft that can move vertically and a connecting rod that links the shaft to the joint on the flexible plate. This arrangement has the inconvenience of not being rigid enough. Also, the deformable wall frequently starts to vibrate when the stream is forced through it. We eliminated the rod and connected the control shaft directly to the joint on the flexible plate. The shaft can slide in the direction of its longitudinal axis in a sleeve and it

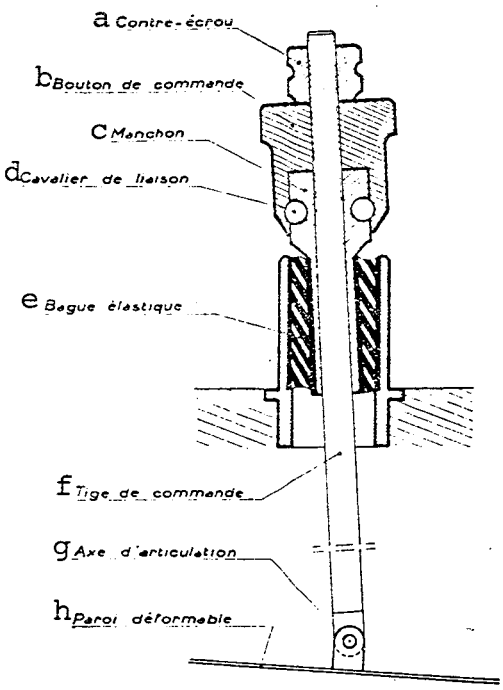

Figure 5
Jack for Controlling the Deformable Walls

Key:
a) Lock Nut
b) Control Button
c) Sleeve
d) Connecting Staple
e) Elastic Ring
f) Control Shaft
g) Joint Axis
h) Deformable Wall

can tilt relative to its initial position because of an elastic ring that is installed between the shaft's sleeve and the chamber's support structure (figure 5). In this way, the two degrees of freedom are assured even though there is no rod. The control button and the head of the sleeve are connected on both sides by inserting a staple through the button. The button is thus maintained at a constant height while the shaft goes up and down. It is possible to rapidly move the control shaft simply by removing the staple and freeing the button.

To allow for the deformation of the flexible plates, one of each plate's ends is fixed while the other is attached to the carriage of a horizontally moving support (figure 6).

The sides of the test chamber /7 and the sonic throat are made of two rectangular glass walls, each of which is mounted in a steel frame. Since the pressure within the airstream is about 0.5 atmosphere, each glass panel has to support a force of approximately 1.5 tonne, which is equal to the weight of the block supporting the chamber. In order to resist such a force, we chose a glass thickness of 30 mm.

Each glass panel opens like a window because of two special hinges with removable pins. To close a panel, it is first folded back against the chamber's braces, then the pins are removed. The panel's frame is thus freed in such a way that a tight contact between

the frames and the chamber's calibrated stringers can be assured through the use of set screws (figure 2).

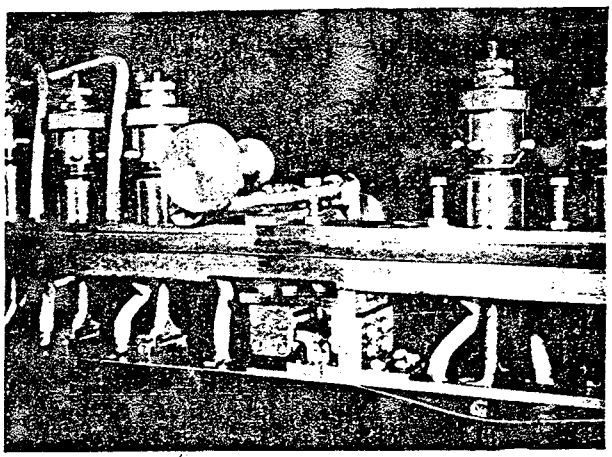

Figure 6
Test Chamber Details

To hold a mockup in the chamber, we planned to replace one of the two solid glass panels with a panel containing a recessed round-bottomed hold. The hole is located on the axis of the airstream, 250 mm from the entrance to the chamber. The mockup, equipped with a locking stud, is lodged in the recessed hole. By exchanging the two glass panels and turning them over, the recessed hole is displaced towards the rear of the chamber, at a distance of 550 mm from the entrance. This arrangement can be adopted when one wants to experiment with the mockup in a supersonic flow after having created a Laval nozzle with the flexible plates at the front of the chamber. So as to be able to exchange the glass panels, we put the hinges for the right panel on the collector and the hinges for the left one on the diffuser.

To permit access to the interior of the channel both upstream and downstream from the test chamber, the plenum chamber's bottom and right side walls open up, and two windows have been installed in the diffuser's side walls.

5. Experimental Results

a) Noises and Vibrations

When the wind tunnel is operating, the noise is easily bearable. In particular, it does not interfere with speech. The test chamber's walls do not vibrate, and the ground vibrations are very slight. They do not rule out the use of optical instruments to visualize the flow.

b) Supersonic Operation

After creating a Laval nozzle with the flexible plates that is calculated to yield an exiting Mach number of 1.5, we were able to start it up and obtain a supersonic flow in the divergent nozzle. One recompression wave was produced in the section where the Mach number attained a value of 1.3.

c) Mach Number Distribution along the Test Chamber

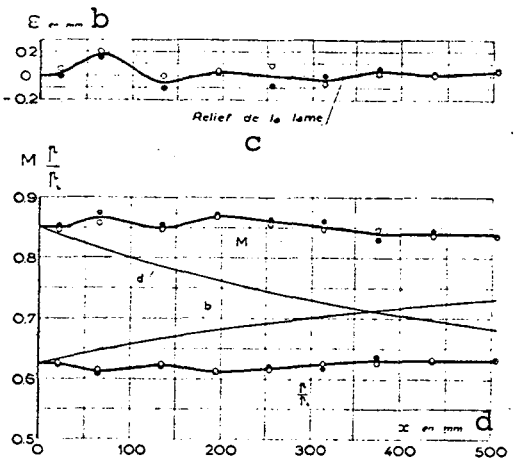

Figure 7
Distribution of Pressure and Mach Number along the Test Chamber Walls

Key: a) Relief of the plate
b) ε in mm
c) x in mm

The pressure p along the rectilinear walls of the airstream, as a fraction of the kinetic pressure p_i, has been represented as a function of the abscissa x measured in the direction of the current and starting at the chamber entrance. The black dots are relative to the top wall, and the white dots to the bottom. The experimental pressure distribution has been represented by taking the average of the results obtained on each of the two walls (figure 7). Curve b gives the pressure distribution calculated on a sectional basis and assuming an isentropic flow. The Mach number M as a function of the ratio p/p_i and for an isentropic flow has been calculated from these two curves: The heavy line corresponds to the experimental pressure curve, and curve d corresponds to curve b. The graph shows that the experimental Mach number is constant to within slightly less than 2%. In the same figure, we have represented the deviation ε of the chamber's flexible walls relative to a line parallel to the axis. A positive deviation here indicates deviation toward the airstream's interior. Note that curve M has an appearance similar to that of the walls' average relief in the interval

$0 < x < 300$ mm. Beyond 300 mm, the walls' relief no longer has any influence; it is overwhelmed by the boundary layer.

d) Use Factor /8

We could not directly measure the wind tunnel's use factor because we did not have a means to measure torque. It was found that the ratio η'_s of the kinetic power in the test section airstream to the electric power supplied was around 2.

We were indirectly able to approximately evaluate the use factor η_s by applying the thermodynamic theory of the air exchanger. When the temperatures have been stabilized, after one hour of operation, the Mach number detected in the rectilinear-walled test chamber is equal to 0.775. Since the percentage of air renewed is 28%, we observe values of $\theta_a = 312°$ and $\theta_i = 350°$ for the absolute temperatures at the exchanger intake and in the plenum chamber, which gives a ratio θ_a/θ_i equal to 0.894. The exchanger chart yields: $\mu = 0.107$, $\lambda = 0.0412$, and $\eta_s = 2.6$ for the use factor. This result also makes it possible to estimate the efficiency η' of the electric motor:

$$\eta' = \frac{\eta'_s}{\eta_s} = \frac{1.96}{2.6} = 0.75$$

Such an efficiency is completely normal for three-phase electric motors.

e) Diffuser Efficiency

The diffuser has parallel top and bottom walls, and its sides form a dihedral angle of 8° 50'. With the goal of eventually improving the wind tunnel's use factor, we have begun to study the diffuser's efficiency. We characterized the flow by two coefficients:

-- The coefficient of pressure increase [1]:

$$\eta_p = \frac{p_2 - p_1}{p_{2*} - p_1}$$

with p_1 and p_2 being the pressures in the entrance and exit sections, p_{2*} the exit pressure in a model diffuser with a reversible flow in which the Mach numbers at the ends are equal to those of the real diffuser and the entrance pressure is p_1.

-- The energy efficiency [1,2]:

$$\eta = \frac{G_2}{G_1}$$

with G being the total usable energy in de Gouy's sense of the term:

$$G = H + \frac{V^2}{2} - \Theta_i S$$

where H is the enthalpy, V the speed, S the entropy, and where the chosen initial temperature is Θ_i, the temperature in the plenum chamber. We take as the zero usable energy level the sum $H_1 - \Theta_i S_1$ relative to the intake, which yields:

$$G_1 = \frac{V_1^2}{2}$$

$$G_2 = \left(H_2 + \frac{V_2^2}{2} - \Theta_i S_2\right) - (H_1 - \Theta S_1)$$

According to Thomson's equation (conservation of $H + V^2/2$), we have:

$$G_2 = \frac{V_1^2}{2} - \Theta_i (S_2 - S_1)$$

The degraded energy is:

$$E_d = G_1 - G_2 = \Theta_i (S_2 - S_1)$$

and the energy efficiency is expressed in the form:

$$\eta = 1 - \frac{E_d}{\frac{V_1^2}{2}}$$

We have found that $\eta_p = 0.797$, and $\eta = 0.800$.

6. Conclusion

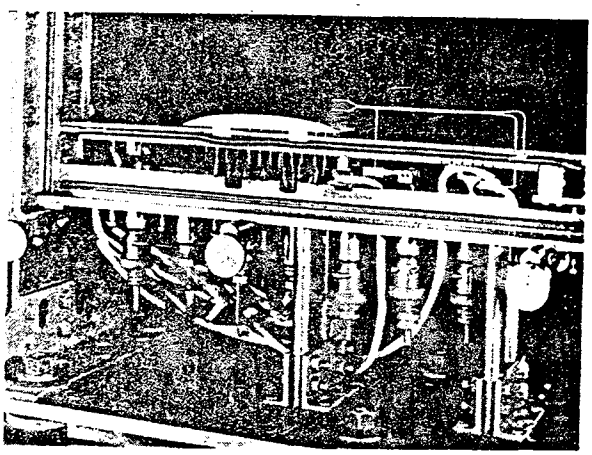

Figure 8
Transonic Bump Experiment

The results obtained show that the wind tunnel at the Lille Institute of Fluid Mechanics makes it possible to conduct research on compressible flows in a domain where the speed is close to that of sound. The wind tunnel is currently being equipped to study the aerodynamic field in the neighborhood of a transonic bump [6] (figure 8).

The wind tunnel possesses many easily controlled small components, which can permit rapid alterations. The airstream is easily accessible. The facility's low power makes its operation inexpensive. Thus, the Lille wind tunnel is a convenient tool for carrying out preliminary work that will guide research done in wind tunnels of larger size.

REFERENCES

1. Bailey, N. P., "Thermodynamics of Air at High Velocities," Journal of the Aeronautical Sciences 11/7, 227-238 (July, 1944).

2. Goethals, R., "Note au sujet des rendements des diffuseurs," [Note Concerning Diffuser Efficiency], Les Cahiers d'Aérodynamique, 5, 120-127 (March-April 1946).

3. Liepmann, H. W., "Interaction between Boundary Layer and Shock Waves in Transonic Flow," Journal of the Aeronautical Sciences, 13/12, 623 (December, 1946).

4. Mondiez, A., Physique industrielle [Industrial Physics], Vol. I, Gauthier-Villars, Paris, 1946, p. 455 (Transmission de la chaleur entre d'eau et l'air) [Transmission of Heat Between Water and Air].

5. Sherwood, A. W., Aerodynamics, McGraw-Hill, New York, p. 45, fig. 4-8.

6. Weaver, J. H., "A method of Wind-Tunnel Testing through the Transonic Range," Journal of the Aeronautical Sciences, 15/1 28-34 (January, 1948).

End of Document